Available online at www.sciencedirect.com
SCIENCE DIRECT®
Catalysis Today 93–95 (2004) 607–613
CATALYSIS TODAY
www.elsevier.com/locate/cattod

Synthesis and acid catalysis of nanoporous silica/alumina-clay composites

Chunhui Zhou*, Xiaonian Li*, Zhonghua Ge, Qinwei Li, Dongsheng Tong

Laboratory of Advanced Catalyst Materials, College of Chemical Engineering, Zhejiang University of Technology, Hangzhou 310014, China

Available online 6 July 2004

Abstract

A novel nanoporous silicoaluminum montmorillonite heterostructured composite (denoted Si/Al-MMT) has been synthesized based on ion exchange and self-assembly techniques. Powder X-ray diffraction (PXRD), thermogravimetric analysis (TGA), transmission electron microscopy (TEM), N_2 adsorption–desorption and Fourier transform infra-red (FTIR) spectroscopy were employed to characterize the synthetic Si/Al-MMT. The synthetic Si/Al-MMT composites exhibit a basal spacing of 3.45 nm, gallery height of 2.39 nm, a BET surface area of 502 m^2/g and silt width of 2.0 nm. The thermal stability of Si/Al-MMT can reach 750 °C. Compared to silica-montmorillonite heterostructured composites (Si-MMT) prepared through the analogous procedures, the thermal stability of Si/Al-MMT was lower due to the pillar formation of mixed oxide structure. The synthetic Si/Al-MMT composites are potentially effective solid acid catalysts for the Friedel–Crafts alkylation of catechol with *tert*-butyl alcohol to synthesize butyl 4-*tert*-butylcatechol (4-TBC). Under experimental condition, the conversion of catechol is 76.8% and the selectivity of 4-TBC is 85.2% over synthetic nanoporous Si/Al-MMT catalysts. Combined with pyridine and ammonium adsorption, the results show that the Lewis acidity can be improved with the addition of aluminum to pillars. Both the acidity and pore structure have effects on the conversion of catechol and the distribution of products.

Keywords: Montmorillonite; Pillared clays; Nanoporous materials; Catalysis; Catechol alkylation; 4-*Tert*-butylcatechol

1. Introduction

Smectite clays have a sandwich structure and their negatively charged aluminaosilicate layers are separated by positively charged cations such as sodium or calcium cations [1]. When large organic and inorganic cations separate the clay sheets, sufficient interlamellar space is created to allow a variety of uses such as adsorbents and catalysts. The intercalation of polynuclear hydroxy metal cations and metal cluster cations in smectites affords pillared clay catalysts with pore sizes that can be larger than those of conventional zeolite catalysts. Such pillaring of layered smectites has given rise to great interests and attempts to transform this abundant mineral into new class of selective heterogeneous catalysts [2]. As an alternative approach to obtain thermally stable porous materials, various inorganic polyoxocations have been intercalated into layered smectite clays, especially ubiquitous montmorillonite. Calcination of these cation-intercalated montmorillonite composites formed inorganic pillared solids with different characteristics, which can be used for separations, sorption and catalysis [3,4].

Although the range of pillared agents has been considerably enlarged, aluminum Keggion ions $[Al_{13}O_4(OH)_{24}]^{7+}$ and silicon cations are often used as pillaring species of which the chemical composition, structure and charge are well identified [5–7]. Pinnavaia reported the introduction of silica in montmorillonite by ion exchange of swollen smectite with silicon acetylacetonate cation ($Si(acac)_3^+$), followed by hydrolysis of the latter. Calcination of the resulting Si $(acac)_3^+$-exchanged smectites resulted in presence of monolayer siloxane chain between the layers with a maximum d_{001} value of 1.26 nm and BET surface area 200 m^2/g [2]. Lewis et al. pillared the montmorillonite with polyhedral oligosilsesquioxane compound, which led to two-layer silica structures between the layers [6]. To date, the application of Al pillared layered clays (Al-PILCs) and Si-PILCs has been severely limited by their thermal stability and pore sizes and distributions. Ge et al. successfully synthesized highly thermal stable Al-pillared montmorillonite by improving pillaring methods [8]. The other appropriate way to improve

* Corresponding authors. Tel.: +86 571 88320062; fax: +86 571 88254568.
E-mail address: catalysis8@yahoo.com.cn (C. Zhou).

0920-5861/$ – see front matter © 2004 Elsevier B.V. All rights reserved.
doi:10.1016/j.cattod.2004.06.014

thermal stability is the introduction of a second component to PILCs during the preparation process [9–11]. For example, Zhao et al. reported the preparation of hydroxysilicoaluminum pillared montmorillonite using Si–Al sol as pillaring agents. The results suggested that the thermal stability and acidity have been increased [12]. To overcome the problem of pore structure, it should be noted that recently a new method have been reported for porous clay heterostructures (PCHs) with narrow pore size distributions in the range of supermicropore to small mesopore (1.4–2.5 nm) [13]. The new approach to designing PCHs is based on the use of intercalated quaternary ammonium cations and neutral amines as co-surfactants to direct the interlamellar hydrolysis and condensation polymerization of neutral inorganic precursor within the galleries of an ionic lamellar solid. Several layered host structures such as fluorohectorite [13], synthetic saponite [14], magadiite [15], and beidellites [16] have been used for conducting analogical synthesis.

In the present paper, our research target is to explore the possibility of the synthesis of silicoaluminum montmorillonite heterostructured composites using ion exchange and self-assembly techniques, in consideration of using gallery-template method to obtain larger pores and using silicoaluminum mixed oxide pillared to improve the thermal stability and acidity of resulting porous clay-based composites. The effects of addition of alumina on structure and properties of clay composites are investigated through comparison with single silica-montmorillonite heterostructured composites, which were successfully prepared by our group recently [17]. The silicoaluminum montmorillonite heterostructured composites are characterized by powder X-ray diffraction, nitrogen adsorption–desorption, transmission electron microscopy and infra-red (IR) techniques. Through the catalytic alkylation reaction of catechol to produce polymerization inhibitor 4-*tert*-butylcatechol, the catalytic properties of porous silicoaluminum montmorillonite heterostructured composites were tested.

2. Experimental

Organic-intercalated montmorillonite (denoted Organo-MMT) was achieved using the <2 μm sodium montmorillonite (Na-MMT, source Clays, from Ningan Zhejiang, China) fractions collected by usual sedimentation. Octadecyltrimethylammonium chloride (ODTA) of 14.6 g in 50 mL deionized water was mixed with a 2% aqueous suspension of 20 g of montmorillonite and the mixture was stirred for 8 h. The solid was filtered, washed and dried at 90 °C. To obtain the silicoaluminum montmorillonite heterostructured composites (denoted Si/Al-MMT, *n*Si/*n*Al = 100:1), 2 g of organic montmorillonite was added to 7.12 g of dodecyl amine. The mixture was stirred for 25 min. Then 60.0 g of tetraethyl orthosilicate (TEOS) and 0.588 g of alumina isopropoxide in 11.6 mL of benzene was added to above reaction mixture under vigorously stirring for 8 h at room temperature. After that, the solid was separated by filtration, aged and finally dried in air on a glass plate and eventually calcined at 540 °C under air for 4 h to removed the template and surfactant. To obtain the silica heterostructured composites (denoted Si-MMT), 5 g of organic montmorillonite was added to a solution of 6.25 g of dodecyl amine. Tetraethyl orthosilicate (TEOS) was added to above reaction mixture under vigorously stirring for 8 h at room temperature. The following procedure is the same as described above. Acidified clays (denoted H-MMT) were prepared by acidifying original sodium montmorillonite at a weight ratio of Na-MMT:H_2O:98% H_2SO_4 of 1:2:0.36 at 100 °C for 4 h. Then the clays were washed with water and dried at 150 °C. The cation exchange capacity of H-MMT was analyzed by conventional Na-exchange and basic titration. The results reveal that the H-MMT has a CEC hydrogen ion of 3.7 mmol/100 g clays with a BET surface area of 164 m^2/g.

Powder X-ray diffraction (PXRD) patterns were measured on a Philips X'Pert diffractometer (Cu Kα radiation). The N_2 sorption isotherms were measured on a macromeritics ASAP 2010C analyzer. Prior to measurements, all samples were outgassed at 300 °C for 4 h under vacuum. Specific surface area was determined by using the BET equation. The pore size distribution was calculated from the desorption curve by Barrett, Joynerand, Hallenda (BJH) method. Thermogravimetric analysis were taken on Shimadzu TG-50 thermal analyzer at a heating rate of 10 °C/min under N_2 flow. Transmission electron microscopy was performed on JEOL 1200EX. The Fourier transform infra-red spectra (FTIR) were recorded on a Shimadzu 8300 spectrometer in a Nujol matrix and the KBr wafer technique was used. The pyridine adsorption infra-red spectra were employed on Digilab FTS-2SPC spectrometer.

The catalytic performances and its acidity were checked by the probe reaction of the alkylation of catechol (CAT) with *tert*-butyl alcohol (TBA) to synthesize 4-*tert*-butylcatechol (4-TBC). The catalytic reactions were carried in a glass batch reactor. The products were analyzed by HPLC with Zoxbax ODS25 ml × 4.6 mm i.d. column and UV detector.

3. Results and discussions

3.1. Formation of nanoporous structure

The corresponding formula for starting Na-montmorillonite is $Na^{+}_{0.66}[Al_{2.97}Fe_{0.37}Mg_{0.66}](Si_{8.00})O_{20}(OH)_4$ with a cation exchange capacity (CEC) of 100 mmol/100 g clay. All samples were characterized by powder X-ray diffraction to trace the change of layered structures. As shown in Fig. 1, each XRD pattern shows the presence of the (0 0 1) reflection peak with the difference of peak width and d_{001} values. The basal spacing d_{001} of starting montmorillonite is 1.29 nm ($2\theta = 7.24^{\circ}$). After calcination at 540 °C, the d_{001} value of the sample decrease to 0.986 nm ($2\theta = 8.96^{\circ}$) which

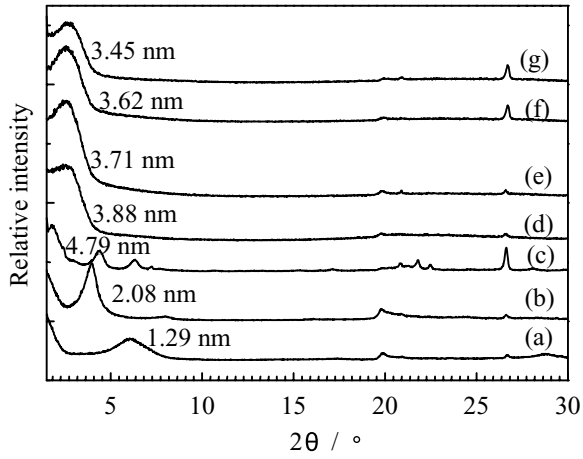

Fig. 1. Powder X-ray diffraction patterns of samples at different stages during synthesis of porous clay-based composites: (a) original MMT; (b) ODTA-MMT; (c) DDA/ODTA-MMT; (d) as-synthesized Si-MMT; (e) Si-MMT after calcinations at 540 °C; (f) as-synthesized Si/Al-MMT; (g) Si/Al-MMT after calcinations at 540 °C.

can be approximately considered as the thickness of each layer of montmorillonite. Octadecyltrimethyl-ammonium cations readily intercalate montmorillonite and increase interlayer distance to 2.08 nm ($2\theta = 4.24°$). As Pinnavaia and co-workers reported for the synthesis of PCHs [14], organic cations with long carbon chain not only changed the character of interlamellar surface from hydrophilic to hydrophobic, but also expanded the gallery to facilitate the accessibility of organic amine and inorganic precursors. The d_{001} increase to 4.79 nm ($2\theta = 1.84°$) after the co-intercalation of DDA. After the intercalation of Si and Si–Al precursors and air-drying, the d_{001} values changes from 4.79 to 3.88 nm and from 4.79 to 3.62 nm, respectively. The changes can be ascribed to the fact that amine and air-drying arouse the interlamellar hydrolysis condensation polymerization of inorganic species. Furthermore, the d_{001} value still keep larger after removal of organic species by calcinations at 540 °C. From this it can be deduced that calcinations arouse formation of pillars within gallery. Upon calcinations at 540 °C for 4 h, the d_{001} value of Si/Al-MMT decreases to 3.45 nm ($2\theta = 2.56°$) which is slightly smaller than d_{001} 3.71 nm ($2\theta = 2.38°$) of Si/MMT. This difference evidences that a certain Si/Al mixed oxide form is present in gallery. So it can be speculated that upon calcinations there is more shrinkage of mixed pillars than pure Si pillars.

As given in Fig. 2 the pore structure of synthetic Si-MMT and Si/Al-MMT composites was investigated by nitrogen adsorption–desorption isotherms. The shape of nitrogen adsorption–desorption isotherms for both samples has a hysteresis loop which belong to a Type-IV isotherms according to the BDDT classification. Furthermore, Si/Al-MMT exhibits larger hysteresis than Si-MMT, and the loop of Si/Al-MMT is of type B and that of Si-MMT is of type A in Bores five types [18,19]. The results indicate the presence of the open slit-shaped pores with parallel walls in Si/Al-MMT and tubular pores in Si/MMT. Namely, Si/Al-MMT and Si-MMT form different pillar structure. Pore size was analyzed by BJH method as shown in Fig. 2(b). Both the gallery height and the pore size in Si/Al-MMT are lower than that of Si-MMT. The Si-MMT has larger distance between pillars and perhaps has formed tubular silica pillar as reported by Agnes et al. [15]. Combined with the shape of loop in isotherms, the pore size of Si/Al-MMT composites should be considered as slit width or the distance between pillars. The detailed structure for two kind pillars is not definite at present. Table 1 shows some characteristics of pore structure for different porous montmorillonite materials. From the data in Table 1, it is discovered that the porosity of Si/Al-MMT composites is greatly increased by intercalation of silicoaluminum. The BET specific surface area of Si/Al-MMT composites reaches 502 m^2/g, with an average pore diameter of 2.0 nm. A dense silica/alumina phase completely filling the interlayer region would not give rise to the observed high surface areas. Further examination of the lattice fringe image spacing by transmission electron microscopy further confirms the expansion of the basal spacing in Si-MMT and Si/Al-MMT. Considering these facts, a new type of nanoporous silicoaluminum montmorillonite heterostructured composites with gallery height 2.39 nm (= 34.5–9.6 nm) is thought to be formed by silicoaluminum intercalation and in situ assembly within gallery. It is also found that the heterostructure by in situ

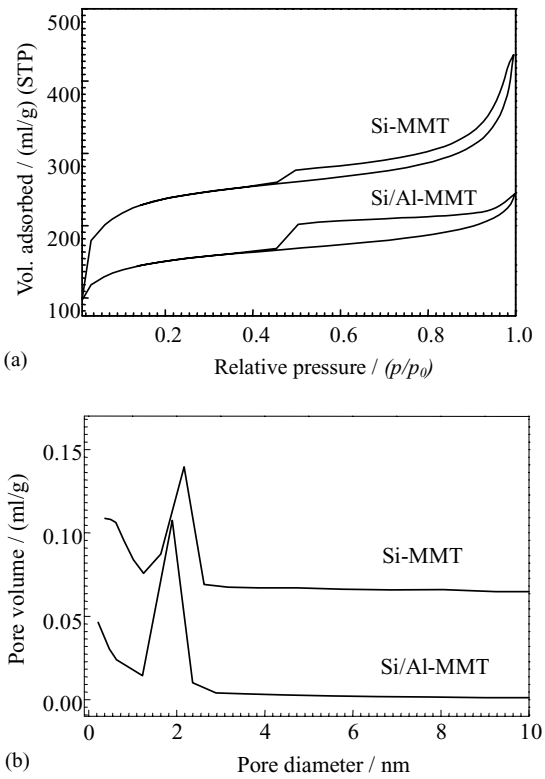

Fig. 2. Nitrogen adsorption–desorption isotherms (a) and pore size distribution curves (b) for synthetic composites.

Table 1
The structure characteristics of different porous montmorillonite-based composites

Sample	d_{001} (nm)	Δd_{001} (nm)	S_{BET} (m^2 g)	Pore size (nm)	Pore volume (mL/g)	Reference
Si-MMT	3.71	2.75	634.4	2.20	0.473	This work
Si/Al-MMT	3.45	2.39	502.6	2.00	0.224	This work
Si-PILCs	1.92	0.97	247	–	0.302	[6]
Al-PILCs	1.81	0.85	221	1.1	–	[8]
Si/Al-PILCs	1.96	1.00	300	–	–	[12]

self-assembly and pillaring has larger BET surface area and pore size than those of PILCs (see Table 1).

3.2. The thermal analysis and thermal stability

The thermogravimetric analysis curves of organo-MMT, as-synthesized Si-MMT and Si/Al-MMT were shown in Fig. 3. The thermogravimetric analysis of organo-MMT revealed about 5% weight loss on heating to 191 °C which can be attributed to elimination of physical adsorbed water. The other two samples show analogous weight loss at the same range of temperature for the same reason. The organo-MMT shows other two parts of weight loss from 200 to 550 °C, owing to decomposition of organic cations and desorption of organic products. Compared with organo-MMT, more distinguishing stages of weight loss is observed in the curve of as-synthesized samples of Si-MMT and Si/Al-MMT and can be divided into three main parts after 200 °C. The first part in temperature ranges 250–342 °C is attributed to the elimination and decomposition of neutral amine and C_{18} surfactant, the second in the range 342–510 °C decreasing slowly is more likely to the removal of residual organic species. The third parts after 700 °C can be ascribed to dehydroxylation of layers and pillars. The thermogravimetric analysis of the as-synthesized Si-MMT and Si/Al-MMT sample revealed about 24% and 26% of weight loss on heating temperature range 250–510 °C, respectively. The percentage of weight loss is much lower than that calculated surfactant quantity in complex $[C_{16}H_{33}N(CH_3)_3]^+_{0.66}[Al_{2.97}Fe_{0.37}Mg_{0.66}](Si_{8.00})O_{20}(OH)_4$ and the experimental weight loss of 32% after 200 °C in the curve of organo-MMT, thus revealing that the intercalation of inorganic precursor and exchange between neutral amine, surfactant and inorganic precursor simultaneously took place. As shown in Fig. 3, the dehydroxylation of OH groups on itself layers of clay only occurred up to 700 °C. It is interesting that two stages of weight loss appear on Si/Al-MMT after 700 °C and only one stage of weight loss takes place for Si-MMT and organo-MMT samples. The phenomenon indicates perhaps there is more obvious dehydroxylation of pillars owing to the Al incorporation and formation of Si/Al mixed pillars.

The thermal stability of the Si/Al-MMT and it is further investigated by powder X-ray diffraction patterns for samples calcined at elevated temperature. As shown in Fig. 4, Si/Al-MMT samples still remain layer structure

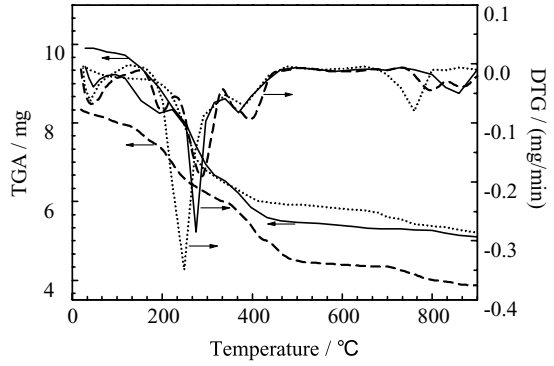

Fig. 3. TG–DTG curves of organo-MMT (dot line), as-synthesized Si-MMT (solid line) and as-synthesized Si/Al-MMT samples (dash line).

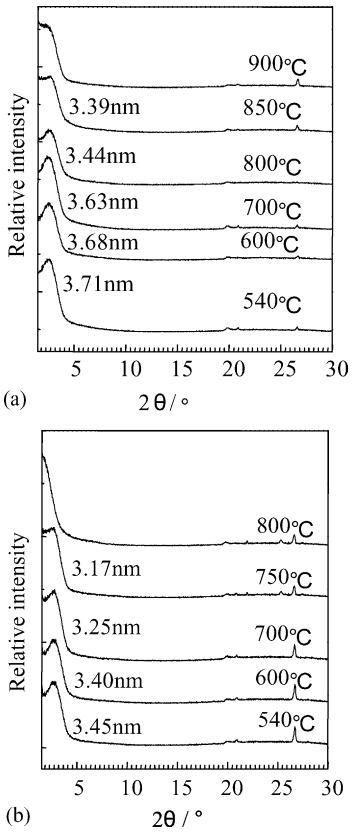

Fig. 4. XRD patterns of montmorillonite-based composites calcined at different temperature: (a) Si-MMT and (b) Si/Al-MMT.

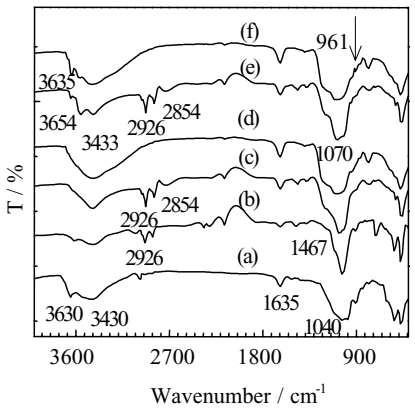

Fig. 5. Infra-red spectra of different clay composites: (a) Na-MMT; (b) ODTA-MMT; (c) as-made Si-MMT; (d) Si-MMT after calcination; (e) as-made Si/Al-MMT; (f) Si/Al-MMT after calcination.

with basal spacing of 3.17 nm ($2\theta = 2.78°$) after calcination at 750 °C for 4 h. The d_{001} peak of Si-MMT can be detected up to 850 °C. The disappearance of d_{001} peak for Si/Al-MMT upon 800 °C and for Si-MMT upon 900 °C is owing to completely layer collapsing. The results suggest that the pillars for Si/Al-MMT are different from that Si-MMT after Al addition. As can be evidenced by XRD patterns in Fig. 1 which show lower gallery height and d_{001} value than that of Si-MMT after calcinations at 540 °C. Though thermal stability of Si/Al-MMT composites was improved in comparison to original MMT and organo-MMT. The thermal stability of Si/Al-MMT is lower than that of Si-MMT because of the Al incorporation and formation of Si/Al complex. The results is good agreement with the results of weight losses after 800 °C as shown in Fig. 3.

3.3. The analysis of infra-red spectra of samples

Infra-red spectroscopy can be clearly used to explore the gallery change at every period of synthesis. The FTIR spectra of samples of organo-MMT, original Na-MMT, Si-MMT and Si/Al-MMT were shown in Fig. 5. In the spectrum of Na-MMT, the peaks at 470, 524, 916, and 1039 cm^{-1} can be ascribed to montmorillonite Si–O bending vibration, Al–O stretching vibration, Al–OH–Al bending vibration and Si–O stretching vibration, respectively. The peaks at 1635, 3430 and 3628 cm^{-1} are assigned to hydration HOH, –OH vibration. Organo-MMT exhibits adsorbed bands of organic groups at 2854, 2926 and 1467 cm^{-1}. The presence of these peaks is considered to be a strong evidence for the intercalation of organic surfactant into the layer of clay. Fig. 5(c)–(f) is the FTIR spectra of as-synthesized Si-MMT, calcined Si-MMT, as-synthesized Si/Al-MMT and calcined Si/Al-MMT, respectively. A stronger band for organic groups is also observed in as-synthesized samples because of amine intercalation. After calcinations, all peaks of organic groups disappeared, thus confirming the organic templates decomposition and elimination. From as-synthesized samples to calcined samples the bands at 3630 cm^{-1} which decrease are attributed to dehydration in interlayer. The new band at 961 cm^{-1} for Si/Al-MMT samples is ascribed to Si–O–Al vibration in the interlayer. Furthermore, the bands at 3635 cm^{-1} which aroused from –OH stretching vibration can only be detected for Si/Al-MMT samples. The results reveal Al incorporation into the pillars, thus illustrating that a new porous material came into being.

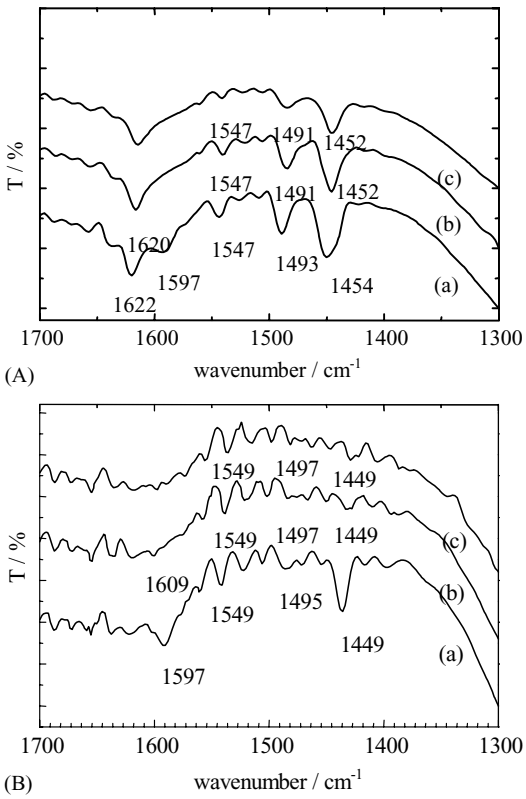

Fig. 6. Infra-red spectra of pyridine adsorbed: (A) Si/Al-MMT and (B) Si-MMT at elevated temperatures: (a) 150 °C; (b) 250 °C; (c) 350 °C.

The type of acid sites (Lewis or Brõnsted) is characterized by adsorption of pyridine monitored by FTIR spectroscopy. As shown in Fig. 6, for both calcined samples of Si-MMT and Si/Al-MMT, the ring stretching frequencies characteristics of pyridine chemisorbed on Lewis acid sites (ca. 1454 cm^{-1}) and on Brõnsted acid sites (ca. 1547 cm^{-1}) are obviously observed. For both samples, Lewis pyridine sites predominate over Brõnsted sites at all elevated temperature. Lewis pyridine sites in Si/Al-MMT are more than that Si-MMT. The results reveal that Si/Al-MMT provides more Lewis acid sites, perhaps arising from a Si–O–Al bond in pillars. With the increase of temperature, Brõnsted sites of Si/Al-MMT decease faster than that of Si-MMT. On the contrary, Lewis acid sites of Si/Al-MMT decreased slightly with elevated temperature. The results seem to show Lewis acid sites are predominantly located on pillars within the interlayer region. Compared with Si-MMT, total number of

Table 2
The acidity and catalytic performances of alkylation reaction over montmorillonite-based catalysts

Catalysts	Si-MMT	Si/Al-MMT	H-MMT
Weak acid sites[a] (mmol/g)	0.081	0.083	0.176
Medium acid sites (mmol/g)	0.572	0.630	0.092
Strong acid sites (mmol/g)	0.097	0.158	1.101
Catalytic activity[b] (%)	68.1	76.8	56.7
Selectivity to 4-TBC (%)	77.6	85.2	56.5
Selectivity to 3-TBC (%)	10.8	8.6	18.4
Selectivity to 3,5-DTBC (%)	11.6	6.2	25.1

[a] Determined by weight loss of ammonia (w_1)/ammonia molecular weight/weight of catalyst sample (w_2).

[b] Reaction temperature = 135 °C; TBA:CAT (molar ratio) = 2:1; solvent: *m*-xylene; reaction time: 8 h; catalysts: 220 mg. 4-TBC: 4-*tert*-butylcatechol; 3,5-DTBC: 3,5-di-*tert*-butylcatechol; 3-TBC: 3-*tert*-butylcatechol.

acid sites for Si/Al-MMT increases owing to the Al addition to pillars.

3.4. The testing of catalytic performances

The possibility of using this materials for shape selective and solid acid catalysis was investigated by probe reaction of alkylation of catechol with *tert*-butyl alcohol produce 4-*tert*-butylcatechol (4-TBC), compared with the H-MMT solid acid catalyst. Catechol alkylation with *tert*-butyl alcohol is a typical Friedel–Crafts alkylation and can be catalyzed by acid sites. Combined with pyridine adsorption infra-red spectra, the acidity feature of experimental catalysts was further checked by ammonia adsorption thermogravimetric analysis. It is clear the H-MMT have more Brõnsted acid sites than the synthetic Si/Al-MMT and Si-MMT, but from the data in Table 2, H-MMT does not exhibit the largest conversion of catechol. The conversion of catechol and 4-TBC to selectivity over the Si/Al-MMT is 76.8 and 85.2%, respectively. From the fact that the Si/Al-MMT possesses better conversion of catechol and 4-TBC to selectivity than Si-MMT, it could be speculated that a significant enhancement of Lewis acidity have effects on both conversion of reactants and selectivity of products. Furthermore, selectivity to 4-TBC over Si/Al-MMT and Si-MMT is both larger than that of H-MMT. It can be partly attributed to more mesoporous structures in Si/Al-MMT and Si-MMT. So it is found that the catalytic performance is governed by both acidity and pore structures. It is clear that the Lewis acidity could obviously be improved by addition of aluminum into pillars, thus leading to improvement of acid catalytic performances.

4. Conclusions

It is very interesting that the silicoaluminum montmorillonite heterostructured composites was gropingly prepared through in situ gallery-template methodology. The results of PXRD, FTIR, TEM and TG reveal that a new type of porous composites is formed by in situ silicon and aluminum intercalation and assembly. The synthetic composites exhibit a basal spacing 3.45 nm, gallery height 2.39 nm, and a BET surface area of 502 m^2/g and silt width 2.0 nm. Compared to silica-montmorillonite heterostructured composites prepared by the analogous procedures, the acidity of Si/Al-MMT was improved owing to the formation of mixed oxide pillars with a slight loss of thermal stability. The synthetic materials are potentially solid acid catalysts for the Friedel–Crafts alkylation of catechol with *tert*-butyl alcohol to synthesize butyl 4-*tert*-butylcatechol (4-TBC). Over synthetic nanoporous silicoaluminum montmorillonite heterostructured composites, the conversion of catechol is 76.8% and the selectivity of 4-TBC is 85.2% under experimental condition. Both the acidity and pore structure has effects on the conversion of catechol and the distribution of products. Although all results have shown the difference between Si pillared heterostructures and Si/Al pillared heterostructures, further systematic research are necessary to identify the exact state within gallery after Al addition so that this novel solid acid catalyst can be developed for industrial application for production of fine chemicals so as to replace polluted liquid acid.

Acknowledgements

Financial supports of Natural Science Foundation of Zhejiang Province of China (No. 201057) are gratefully acknowledged. The carefully revision for English to this manuscript by Dr. Ge M. in USA are sincerely acknowledged.

References

[1] R.E. Grim, Clay Mineralogy, 3rd ed., McGraw-Hill Book Co., New York, 1968.
[2] T.J. Pinnavaia, Science 220 (1983) 365.
[3] F. Figueras, Catal. Rev. Sci. Eng. 30 (1988) 457.
[4] A. Vaccari, Appl. Clay Sci. 14 (1999) 161.
[5] H.J. Chae, I.-S. Nam, S.W. Ham, S.B. Hong, Catal. Today 68 (2001) 31.
[6] R.M. Lewis, K.C. Ott, R.A. Van Santen, US Patent 4 510 257 (1985).
[7] C.X. Guo, W.H. Hou, M. Guo, Q.J. Yan, Y. Chen, Chem. Commum. (1997) 801.
[8] Z.H. Ge, T.J. Pinnavaia, Cuihua Xuebao (China) 16 (1995) 222.
[9] A. Gil, M.L. Gandia, M.A. Vicente, Catal. Rev. Sci. Eng. 42 (2000) 145.
[10] H. He, L. Zhang, J. Klinowski, M.L. Occelli, J. Phys. Chem. 99 (1995) 6980.
[11] J.-H. Choy, J.-H. Park, J.-B. Toon, Bull. Kor. Chem. Soc. 19 (1998) 1185.
[12] D.Y. Zhao, Y.S. Yang, X.X. Guo, Inorg. Chem. 31 (1992) 4727.
[13] A. Galarneau, A. Barodawalla, T.J. Pinaavaia, Nature 375 (1995) 529.
[14] M. Polverejan, Y. Liu, T.J. Pinnavaia, Stud. Surf. Sci. Catal. 129 (2000) 401.

[15] F. Agnes, K. Imre, S.-I. Niwa, M. Toba, Y. Kiyozumi, F. Mizukami, Appl. Catal. A 176 (1999) 153.
[16] J.A. Martens, E. Benazzi, J.B. Rendle, S. Lacombe, R.L. Dred, Stud. Surf. Sci. Catal. 130 (2000) 293.
[17] C.H. Zhou, Q.W. Li, Z.H. Ge, X.N. Li, Frontier of Solid State Chemistry, World Scientific, Singapore, 2002, p. 275.
[18] J.R. Anderson, K.C. Pratt, Introduction to Characterization and Testing of Catalysis, Academic Press, Australia, 1985, p. 113–114.
[19] J.H. de Bore, in: D.H. Everett, F.S. Stone (Eds.), The Structure and Properties of Porous Materials, Butterworths, London, 1958, p. 68.